Original Article

Reduced Access to Insulin-Sensitive Tissues in Dogs With Obesity Secondary to Increased Fat Intake

Martin Ellmerer,[1,2] Marianthe Hamilton-Wessler,[1] Stella P. Kim,[1] Katrin Huecking,[1] Erlinda Kirkman,[1] Jenny Chiu,[1] Joyce Richey,[1] and Richard N. Bergman[1]

Physiological hyperinsulinemia provokes hemodynamic actions and augments access of macromolecules to insulin-sensitive tissues. We investigated whether induction of insulin resistance by a hypercaloric high-fat diet has an effect on the extracellular distribution of macromolecules to insulin-sensitive tissues. Male mongrel dogs were randomly selected into two groups: seven dogs were fed an isocaloric control diet (~3,900 kcal, 35% from fat), and six dogs were fed a hypercaloric high-fat diet (~5,300 kcal, 54% from fat) for a period of 12 weeks. During hyperinsulinemic-euglycemic clamps, we determined transport parameters and distribution volumes of [^{14}C]inulin by applying a three-compartment model to the plasma clearance data of intravenously injected [^{14}C]inulin (0.8 μCi/kg). In another study with direct cannulation of the hindlimb skeletal muscle lymphatics, we investigated the effect of physiological hyperinsulinemia on the appearance of intravenously injected [^{14}C]inulin in skeletal muscle interstitial fluid and compared the effect of insulin between control and high-fat diet groups. The hypercaloric high-fat diet resulted in significant weight gain (18%; $P < 0.001$) associated with marked increases of subcutaneous (140%; $P < 0.001$) and omental (83%; $P < 0.001$) fat depots, as well as peripheral insulin resistance, measured as a significant reduction of insulin-stimulated glucose uptake during clamps (−35%; $P < 0.05$). Concomitantly, we observed a significant reduction of the peripheral distribution volume of [^{14}C]inulin (−26%; $P < 0.05$), whereas the vascular distribution volume and transport and clearance parameters did not change as a cause of the diet. The second study directly confirmed our findings, suggesting a marked reduction of insulin action to stimulate access of macromolecules to insulin-sensitive tissues (control diet 32%, $P < 0.01$; high-fat diet 18%, NS). The present results indicate that access of macromolecules to insulin-sensitive tissues is impaired during diet-induced insulin resistance and suggest that the ability of insulin itself to stimulate tissue access is diminished. We speculate that the observed diet-induced defects in stimulation of tissue perfusion contribute to the development of peripheral insulin resistance. *Diabetes* 55:1769–1775, 2006

Besides its effect to stimulate glucose uptake at the cellular level, insulin can regulate blood flow (1–5) as well as alter perfusion of insulin-sensitive tissues (6–8). Rattigan et al. (9) reported that insulin recruits microvascular vessels in skeletal muscle, changing flow distribution independent of its effect to alter total blood flow. Clark et al. (10) suggested that insulin's microvascular actions contribute to its overall effect on nutrient and hormone delivery to skeletal muscle. Yet the importance of insulin's hemodynamic effects to the regulation of in vivo insulin action remains unclear.

In a recent study (8), we introduced an alternative approach to examine the effects of physiological insulin concentrations on perfusion of insulin-sensitive tissues. We measured the effect of systemic insulin infusion on transport and distribution kinetics of the extracellular marker [^{14}C]inulin in an animal model that allowed access to hindlimb lymph, a surrogate for interstitial fluid. Insulin, at physiological concentrations, augments the access of the labeled inulin to insulin-sensitive tissues. The latter study supported the concept that the in vivo effect of insulin is determined, at least in part, by insulin's own effect to reach metabolically active tissues by changing local blood flow distribution patterns.

The question remains whether insulin resistance can be attributed to alterations in the blood flow–altering effects of the peptide. The objective of the present study was to test whether the hypercaloric induction of fat-induced peripheral insulin resistance alters perfusion of insulin-sensitive tissues. In fact, our results suggest reduced tissue perfusion of [^{14}C]insulin after induction of diet-induced insulin resistance in dogs. These studies implicate changes in tissue perfusion in the etiology of nutritive fat-induced insulin resistance.

RESEARCH DESIGN AND METHODS

Experiments were performed in male mongrel dogs (n = 13, 27.5 ± 5.4 kg body wt [means ±SD]). Animals were housed under controlled kennel conditions (12-h light/dark cycle) in the University of Southern California Medical School Vivarium. Animals were accepted into the study only if judged by the veterinary staff to be in good health. One week before experimentation, under general anesthesia, chronic catheters were implanted. Catheters were placed in the carotid artery for sampling of arterial blood and into the left jugular and femoral veins for infusions. On the morning of conscious experiments, an acute catheter was inserted into the saphenous vein for the variable infusion of glucose and for the injection of [^{14}C]inulin. All experimental protocols were approved by the University Institutional Animals Care and Use Committee.

From the [1]Department of Physiology and Biophysics, University of Southern California School of Medicine, Los Angeles, California; and the [2]Medical University Graz, Department of Internal Medicine, Diabetes and Metabolism, Graz, Austria.

Address correspondence and reprint requests to Richard N. Bergman, PhD, Keck Professor of Medicine, Department of Physiology and Biophysics, University of Southern California School of Medicine, 1333 San Pablo St., MMR 626, Los Angeles, CA 90033. E-mail rbergman@usc.edu.

Received for publication 18 November 2005 and accepted in revised form 16 March 2006.

MRI, magnetic resonance imaging.

DOI: 10.2337/db05-1509

Diets and general procedure. Before entering the study protocol, dogs were randomly separated into two groups (control $n = 7$, fat fed $n = 6$). During a 3-week period, all 13 dogs were given a control diet including one daily can (415 g) of Hill's Prescription Diet (9% protein, 8% fat, 10% carbohydrates, and 73% moisture [Hill's Pet Nutrition, Topeka, KS]) and ~825 g dry diet (26.4% protein, 14.7% fat, 39.6% carbohydrates, 2.9% fiber, and 16.5% moisture [Wayne Dog Food; Alfred Mills, Chicago, IL]). Thus, the total control diet consisted of ~3,900 calories: 27% from proteins, 35% from fat, and 39% from carbohydrates. In all animals during the 3-week control period, magnetic resonance imaging (MRI) scans and euglycemic clamp experiments were performed.

Control animals. Besides an MRI scan and euglycemic clamps performed during the control period, in the seven control animals, after the 3-week control diet, a terminal inulin kinetics experiment was performed under general anesthesia (study 2).

Animals fed the high-fat diet. After 2–3 weeks on the control diet, during which euglycemic clamps (study 1) and MRIs were performed, dogs ($n = 6$) were given an hypercaloric high-fat diet for a period of 12 weeks. This diet consisted of the control diet supplemented with 6 g/kg body wt of cooked bacon grease supplied by the University of Southern California Keck School of Medicine cafeteria. This change increased the calories to ~5,300, with 19% from proteins, 54% from fat, and 27% from carbohydrates. After the 12-week period, MRI scans and euglycemic clamp experiments (study 1) were repeated. In addition, after 12 weeks, the terminal inulin distribution procedure (study 2) was performed in the fat-fed animals.

MRI. MRI scans were performed as described previously (11). Preanesthesia was induced with subcutaneous injection of acepromazine (0.1 mg/kg body wt [Bio-ceutic, St. Joseph, MO]) and atropine sulfate (0.04 mg/kg body wt, 1/120 grain [Western Medical Supply, Arcadia, CA]), followed by intravenous anesthesia with ketamine HCl (10 mg/kg [Phoenix Pharmaceutical, St. Joseph, MO] and diazepam (0.2–0.5 mg/kg [Abbott Laboratories, North Chicago, IL]). Thirty 1-cm axial abdominal images (T1 slices; TR:500 TE:14) were obtained using a General Electric 1.5 Tesla Horizon magnet. The images were analyzed using ScionImage (Windows 98 Version Beta 4.0.2; Scion, Frederick, MD), which quantified nonfat tissue (pixel value 0–120) and fat tissue (pixel value 121–255) in each slice. Total trunk fat and tissue were estimated as the integrated fat or tissue across all 30 slices. Percent fat was then calculated as the total trunk fat divided by the total trunk tissue. Omental fat was defined as fat within the peritoneal cavity, integrated from ±5 slices at the level at which the left renal artery branches from the aorta. Percent omental fat was defined as the omental fat devided by the total tissue volume from the same 10 slices.

Study 1: hyperinsulinemic-euglycemic clamp before (week 0) and after (week 12) high-fat diet–induced insulin resistance. Whole-body and peripheral insulin action as well as [^{14}C]inulin distribution kinetics were estimated at physiologically elevated insulin concentrations. The experiments started at 0700 in the morning. At −150 min, a primed infusion of [3-^{3}H]glucose was initiated into the femoral vein catheter (priming dose 25 μCi, infusion 0.25 μCi/min; DuPont-NEN, Boston, MA) and was maintained throughout the study protocol. Beginning at 0 min, somatostatin (1.0 μg · min^{-1} · kg^{-1}; Bachem, Torrance, CA) was infused to suppress endogenous insulin secretion. Canine insulin (6 pmol · min^{-1} · kg^{-1}; Novo Nordisk, Bagsvaerd, Denmark) was infused for a period of 5 h, until the end of the experiment at 300 min. Glucose was measured in 10-min intervals during the first 60 min and in 15-min intervals thereafter, and plasma glucose was clamped to basal level by variable infusion of 50% glucose spiked with 2.7 μCi/mg [3-^{3}H]glucose (12). After steady-state plasma insulin concentrations were achieved at 120 min, an intravenous bolus of [^{14}C]inulin was given into a saphenous vein, and samples for the measurement of the kinetic profile of [^{14}C]inulin were collected at 1, 2, 3, 4, 5, 6, 8, 10, 12, 15, 17, 20, 25, 30, 35, 40, 45, 50, and 60 min and in 15-min intervals until the end of the experiment at $t = 300$.

Study 2: two-step hyperinsulinemic-euglycemic clamp with interstitial fluid access in control dogs (control) and dogs after 12 weeks on a high-fat diet (fat fed). A euglycemic-hyperinsulinemic clamp under general anesthesia was performed in the control dogs after ~3 weeks on control diet (control) and in fat-fed dogs after 12 weeks on the high-fat diet (fat fed) to enable sampling of the deep hindlimb lymph as previously described (13). Results from experiments of the control diet have been reported recently and are included here as controls (8). Surgery was performed at 0700. Dogs were preanesthetized with acepromazine maleate (0.22 mg/kg Prom-Ace; Aueco, Fort Dodge, IA) and atropine sulfate (0.11 ml/kg; Western Medical). Anesthesia was induced with sodium pentobarbital (0.44 ml/kg Nembutal; Abbott Laboratories) and was maintained with halothane and nitrous oxide. Indwelling catheters were implanted in the left carotid artery (sampling) and left or right jugular vein (saline drip). Left and right cepahlic vein intracatheters were inserted for infusions as detailed below. Left hindlimb muscle lymphatic fluid was sampled via a small polyethylene catheter (PE10 to PE90, predominantly PE50) inserted into a deep lymph vessel (13). Blood pressure, heart rate, and respiratory CO_2 were continuously monitored. Animals received a saline drip throughout both the surgery and the experiment (~1 l was administered during the first 60 min of surgery and a slow drip thereafter). After experiments, animals were killed by an overdose of sodium pentobarbital (65 mg/kg Eutha-6; Western Medical).

The experimental protocol consisted of three temporal phases: a basal replacement phase (−300 to 0 min), an insulin activation phase (0–300 min), and an insulin deactivation phase (300–420 min). At −300 min, a primed (25 μCi) tracer infusion of high-performance liquid chromatography–purified [3-^{3}H]-D-glucose (0.25 μCi/min; DuPont-NEN) was started and maintained throughout the study to assess glucose turnover. At the same time (−300 min) a continuous infusion of somatostatin (1.0 μg · min^{-1} · kg^{-1}; Bachem, Torrance, CA) was started to suppress endogenous insulin release and a basal replacement infusion of canine (porcine) insulin (1.2 pmol · min^{-1} · kg^{-1}; Novo Nordisk) was initiated. Both the somatostatin and the replacement insulin infusion were maintained throughout the study. From −300 min until the end of the experiment (420 min), arterial glucose was clamped at basal levels by exogenous infusion of 50% glucose labeled with [3-^{3}H]-D-glucose (2.7 μCi/g glucose) (12). We have previously shown that femoral blood flow, glucose infusion rate, and glucose turnover are constant for a 12-h glucose clamp, demonstrating that the anesthetized dog preparation is stable for the time of these experiments. After steady-state replacement, insulin levels were established; at time −180 min, an intravenous bolus of [^{14}C]inulin (4 μCi/kg body wt; American Radiolabeled Chemicals, St. Louis, MO) was administered to quantify transport and distribution kinetics of [^{14}C]inulin in arterial plasma and hindlimb lymph for a period of 3 h. At time 0 min, a primed intravenous infusion of insulin (6 pmol · min^{-1} · kg^{-1}; Novo Nordisk) was started and maintained for a period of 5 h. At time 120 min, after steady-state insulin concentrations were established, a second intravenous bolus of [^{14}C]inulin (4 μCi/kg body wt) was given. At time 300 min, or 5 h after the start of the primed insulin infusion, the insulin infusion was terminated, and the clearance of insulin from plasma and hindlimb lymph was measured for 2 h or until 420 min, when the experimental protocol ended. Arterial sampling (~4 ml blood) was coupled with hindlimb lymph sampling (continuously from ~2 min before to ~2 min after arterial sample time). For the first 60 min after insulin activation and deactivation and after the [^{14}C]inulin boluses, arterial blood samples were drawn according to the schedule as described for study 1; hindlimb lymph samples were taken in 5-min intervals during these periods. For the remainder of the experimental protocol, both arterial plasma and hindlimb lymph samples were taken in 15-min intervals. Weekly overnight fasting plasma samples were obtained from all dogs on a nonexperimental day at 0700.

Assays. Arterial blood samples for assay of glucose, insulin, [3-^{3}H]glucose, and [^{14}C]inulin as well as hindlimb lymph samples for assay of porcine insulin and [^{14}C]inulin were collected in microtubes precoated with lithium-heparin (Becton Dickinson, Franklin Lakes, NJ). Arterial sample tubes were additionally precoated with EDTA (Sigma Chemicals, St. Louis, MO). Blood samples were centrifuged immediately, the supernatant transferred, and, after measurement of plasma glucose, stored at −20°C until further assay. Hindlimb lymph samples were stored at −20°C immediately after sampling. Online plasma glucose was assayed using glucose oxidase on an automated analyzer (model 23A; Yellow Springs Instruments, Yellow Springs, OH). Porcine insulin was measured in plasma with an enzyme-linked immunosorbent assay. Samples for the analysis of [3-^{3}H]glucose were deproteinized using barium hydroxide and zinc sulfate as previously described (14). For the determination of [^{14}C]inulin in plasma and hindlimb lymph samples, 0.15 ml of sample was mixed with 1 ml tissue solubilizer (NCS; Beckman, Fullerton, CA). After a 30-min incubation at room temperature, samples were counted in 10 ml of Ready Organic scintillation fluid (Beckman) on a dual-channel liquid scintillation counter (Beckman). Weekly fasting samples for the analysis of glucose, lactate, and insulin were precoated with lithium fluoride and heparin (Brinkmann Instruments, Westbury, NY) containing 50 μl of EDTA; samples for nonesterified fatty acid and glycerol were taken in tubes with EDTA and tetrahydrolipstatin to inhibit in vitro lipase activity (15). All samples were kept on ice immediately after sampling.

Pharmacokinetic data analysis and [^{14}C]inulin distribution model. Distribution and elimination of inulin was accurately described using a three-compartment model as originally proposed by Henthorn et al. (16) and recently confirmed and applied by us (8,17). Henthorn et al. characterized the distribution of inulin in extracellular space by a three-compartmental model with a central compartment representing the plasma volume (V_1) and a slow (V_2) and a rapid (V_3) equilibrating compartment representing the interstitial fluid space. The faster equilibrating compartment is generally assumed to be supplied by capillaries in the splanchnic bed that are porous and lack a continuous investment of the basement membrane, while skeletal muscle is assumed to account for a major component of the slowly equilibrating interstitial fluid compartment. Parameter k_{01} represents the irreversible

TABLE 1
Body composition and basal metabolic parameters: effects of a high-fat diet on body composition and fasting plasma characteristics

	Body wt (kg)	Total fat (%)	Omental fat* (cm^3)	Subcutaneous* fat (cm^3)	Glucose (mg/dl)	Lactate (mg/dl)	Insulin (pmol)	NEFA (pmol)	Glycerol (pmol)
Week 0	29 ± 3	18 ± 4	332 ± 62	249 ± 119	90 ± 2	11 ± 3	54 ± 5	0.47 ± 0.03	0.9 ± 0.1
Week 12	34 ± 2	34 ± 4	607 ± 93	595 ± 160	92 ± 2	11 ± 2	120 ± 7	0.60 ± 0.05	1.2 ± 0.3
P	$P < 0.001$	$P < 0.001$	$P < 0.001$	$P < 0.001$	NS	NS	$P < 0.001$	$P = 0.06$	NS

Data are means ± SE. Dogs were investigated after 3 weeks on a control diet (week 0) and after 12 weeks on a hypercaloric high-fat diet (week 12). *Omental fat and subcutaneous fat, calculated as fat within and outside the peritoneal cavity in a 11-cm region of the thorax, using the slice at the level where the left renal artery braches from the abdominal aorta as a midpoint landmark. NEFA, nonesterified fatty acid.

clearance of inulin from the plasma compartment by the kidney (16,18), and transport between plasma and slow (k_{21}, k_{12}) and rapid (k_{31}, k_{13}) equilibrating compartments occurs by passive diffusion ($k_{12} \times V_2 = k_{21} \times V_1 = CL_2$; $k_{13} \times V_3 = k_{31} \times V_1 = CL_3$) (16). [^{14}C]inulin does not reach intracellular space. Under these assumptions, the equations describing the three-compartment model are as follows:

$$\frac{dc_1}{dt} = -(k_{01} + k_{21} + k_{31})c_1 + k_{21}c_2 + k_{31}c_3 \quad (1)$$

$$\frac{dc_2}{dt} = k_{21}\frac{V_1}{V_2}(c_1 - c_2) \quad (2)$$

$$\frac{dc_3}{dt} = k_{31}\frac{V_1}{V_3}(c_1 - c_3) \quad (3)$$

with V_i as volume and c_i as concentration of compartment I. With the initial conditions, $c_1(0) = \frac{BOLUS}{V_1}$, $c_2(0) = 0$, and $c_3(0) = 0$ the six parameters, V_1, V_2, V_3, k_{01}, k_{21}, and k_{31} are a priori identifiable. Parameters k_{12} and k_{13} can be derived from the diffusion assumptions. Distribution volumes were expressed as milliliters per kilogram body weight, and clearance and tissue-specific transport parameters were expressed as milliliters per minute ($CL_{01} = k_{01} \times V_1$, $CL_2 = k_{21} \times V_1$, $CL_3 = k_{31} \times V_1$). Model parameters of study 1 and study 2 were analyzed using plasma data only. The hindlimb lymph data of study 2 were used to confirm the model-predicted differences of the response of the slow equilibrating interstitial fluid compartment.

Numerical methods and data analysis. Data are reported as means ± SE. Paired Student's *t* tests have been used to calculate statistical significance within and between subsets of data, respectively. *P* values are reported with values <0.05 considered significant. Statistical data analysis has been performed using Minitab (State College, PA) and Excel (Microsoft) software. Parameter identification for both models was obtained using a modified Gauss-Newton algorithm with inverse variance weights. Accuracy of individual parameter estimates was evaluated as a fractional standard deviation. Model parameters were identified using the Windows version of the SAAM program (National Institutes of Health, Bethesda, MD) implemented on a personal computer.

RESULTS

Body composition. The hypercaloric high-fat diet provoked a significant increase in body weight of ~18% ($P < 0.001$), with most (15%) occurring by week 6. Trunk fat increased 87% ($P < 0.001$). Thus, the hypercaloric high-fat diet resulted in increased trunk adiposity, which was accommodated by a substantial increase in body weight. To differentiate between increases in omental versus subcutaneous fat depots, MRI scans of a defined axial region of the trunk were analyzed. After 12 weeks on the high-fat diet, a significant increase of both fat depots was observed (Table 1)

Basal metabolic parameters. Despite the almost twofold increase in total trunk adiposity, we observed no significant change in fasting glucose (90 ± 2 to 92 ± 2 pmol/l, $P > 0.5$). Also, fasting lactate and glycerol concentrations were comparable before and after the high-fat diet, whereas a tendency for an increased fasting nonesterified fatty acid concentration (+26%; $P = 0.06$) was observed. In contrast to unchanged fasting glucose, a highly significant, over twofold increase in fasting insulin was observed (54 ± 5 to 120 ± 7 pmol/l, $P < 0.001$). Thus, the hypercaloric high-fat diet resulted in fasting hyperinsulinemia, despite no change in fasting glucose.

Study 1: hyperinsulinemic-euglycemic clamp before (week 0) and after (week 12) high-fat diet–induced insulin resistance. High-fat diet caused peripheral and hepatic insulin resistance. Steady-state glucose disposal was reduced by 35% ($P < 0.05$). Endogenous glucose production was less suppressed by insulin after 12 weeks (week 0: 11.9 ± 5.6% of basal; week 12: 41.3 ± 5.0% of basal; $P < 0.01$) (Table 2). As previously demonstrated (8), insulin enhances the extracellular distribution volume of the macromolecule inulin. In study 1, we tested whether the induction of insulin resistance may alter the distribution kinetics of [^{14}C]inulin during systemic hyperinsulinemia. Despite similar hyperinsulinemia (week 0: 413 ± 35 vs. week 12: 482 ± 62 pmol/l; NS), the pattern of disappearance of inulin was altered significantly after the fat diet (Fig. 1*A*). Whereas the plasma volume and all transport and clearance parameters remained unchanged before versus after the high-fat diet (Table 3), we found a substantial and significant decrease in size of the slower compartment (V_2) for distribution of inulin (−26 ± 9%; $P < 0.05$) (Fig. 1*B*). Therefore, feeding a hypercaloric high-fat diet reduced the ability of insulin per se to provide access of macromolecules to insulin-sensitive tissues.

TABLE 2
Steady-state characteristics: study 1. Results of hyperinsulinemic-euglycemic clamp experiment in dogs investigated after 3 weeks on a control diet (week 0) and after 12 weeks on a hypercaloric high-fat diet (week 12)

	Glucose (mg/dl)	Insulin (pmol)	Glucose infusion rate ($mg \cdot min^{-1} \cdot kg^{-1}$)	Glucose uptake ($mg \cdot min^{-1} \cdot kg^{-1}$)	Glucose production ($mg \cdot min^{-1} \cdot kg^{-1}$)	S_{iCLAMP}*
Week 0	100.2 ± 1.2	413 ± 35	11.8 ± 1.3	12.3 ± 1.3	0.12 ± 0.26	2.8 ± 0.4
Week 12	100.0 ± 0.6	482 ± 62	7.1 ± 0.6	7.9 ± 0.5	0.93 ± 0.13	1.6 ± 0.3
P	NS	NS	$P < 0.05$	$P < 0.05$	$P < 0.05$	$P < 0.05$

Data are means ± SE. *Insulin sensitivity [$(dl \cdot min^{-1} \cdot kg^{-1} \cdot pmol^{-1}) \times 10^5$]; glucose uptake and production and insulin sensitivity determined from [3-^{3}H]glucose tracer analysis.

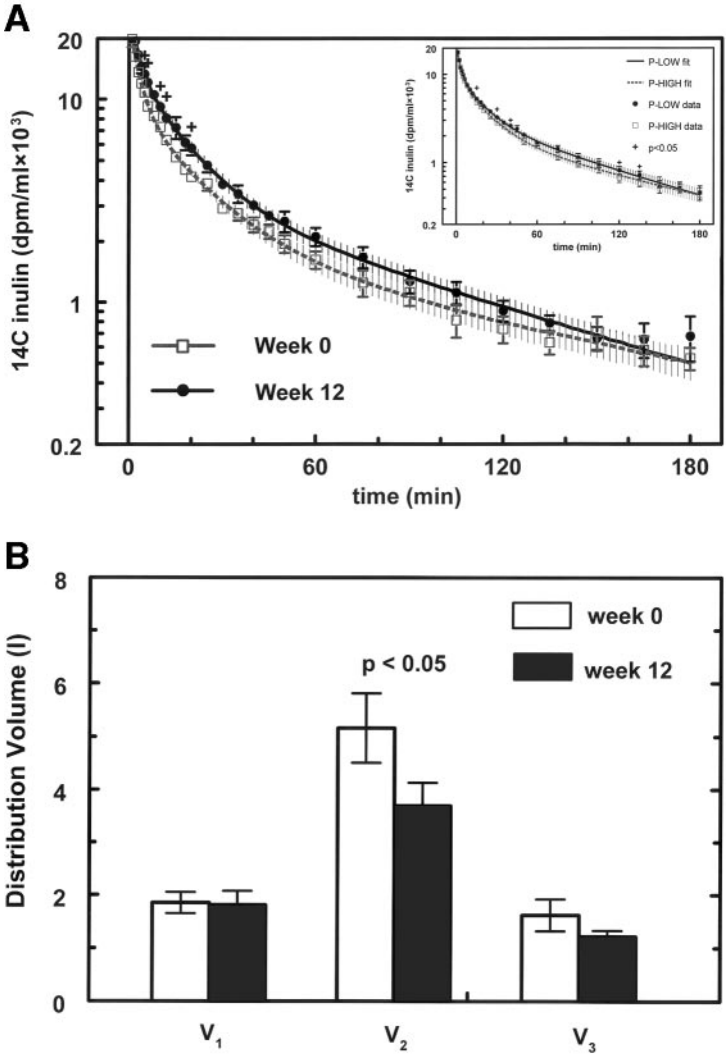

FIG. 1. Results from study 1. *A*: Plasma clearance of [^{14}C]inulin for dogs before (□) and after (●) 12 weeks on the hypercaloric high-fat diet at physiologically elevated plasma insulin concentrations. Small graph indicates similar plasma clearance of [^{14}C]inulin at low plasma insulin concentrations compared with clearance after the high-fat diet (both ●). Lines indicate respective plasma clearance as suggested by compartmental modeling analysis. Vertical lines indicate 95% CI. *B*: Model-predicted distribution volumes before (week 0) and after (week 12) 12 weeks on the hypercaloric high-fat diet. Data are means ± SE.

Study 2: two-step hyperinsulinemic-euglycemic clamp with interstitial fluid access in control dogs (control) and dogs after high-fat diet–induced insulin resistance (fat fed). Study 1 concluded from plasma inulin kinetics alone that fat feeding impaired insulin's effect to enhance macromolecules' access to slowly equilibrating tissues. To investigate whether these tissues were indeed insulin sensitive, we determined the distribution kinetics of the extracellular marker at two different levels of plasma insulin and sampled hindlimb lymph in an anesthetized dog preparation. Similar to study 1, steady-state characteristics indicated development of both hepatic and peripheral insulin resistance in dogs fed the hypercaloric high-fat diet compared with a control group (Table 4). Whereas in control animals, physiological hyperinsulinemia stimulated the slow distribution compartment of [^{14}C]inulin (+32%; $P < 0.01$), this effect was only halfmaximal (+18%; NS) in fat-fed dogs and did not reach statistical significance (Fig. 2). Similar to the control experiments, no significant changes in the plasma distribution volume or any of the clearance parameters were observed in dogs fed a hypercaloric high-fat diet (Table 5). Reduced effect of insulin to stimulate tissue recruitment of [^{14}C]inulin was also indicated from the hindlimb lymph response to the intravenous [^{14}C]inulin bolus. Whereas significant differences of the response between low and high plasma insulin levels were observed for both groups, this difference was attenuated in dogs fed the high-fat diet (Fig. 3). Insulin concentrations in plasma (Table 4) and interstitial fluid of skeletal muscle (control low insulin 52 ± 5 pmol/l,

TABLE 3
Model parameters: study 1. Effects of a high-fat diet on distribution kinetics of [^{14}C]inulin: results from a hyperinsulinemic-euglycemic clamp experiment as performed before (week 0) and after (week 12) a hypercaloric high-fat diet in dogs

	V_1 (l)*	V_2 (l)*	V_3 (l)*	CL_{01} (ml/min)	CL_2 (ml/min)	CL_3 (ml/min)
Week 0	1.9 ± 0.2	5.2 ± 0.7	1.6 ± 0.3	104 ± 13	74 ± 5	270 ± 54
Week 12	1.8 ± 0.3	3.7 ± 0.4	1.2 ± 0.1	109 ± 10	82 ± 6	319 ± 73
P	NS	$P < 0.05$	NS	NS	NS	NS

Data are means ± SE. *Distribution volumes are indicated in liters instead of milliliters per kilogram body weight to account for the weight change during the diet (see Table 1). CL_{01}, CL_2, and CL_3 indicate clearance and tissue-specific transport.

TABLE 4
Steady-state characteristics from study 2: results of hyperinsulinemic-euglycemic clamp experiment in anesthetized dogs

	Glucose (mg/dl)		Insulin (pmol)		Glucose infusion rate ($mg \cdot min^{-1} \cdot kg^{-1}$)		Glucose uptake ($mg \cdot min^{-1} \cdot kg^{-1}$)		Glucose production ($mg \cdot min^{-1} \cdot kg^{-1}$)	
Clamp period infusion rates ($mU \cdot min^{-1} \cdot kg^{-1}$)	0.2	1.2	0.2	1.2	0.2	1.2	0.2	1.2	0.2	1.2
Control	99.5 ± 1.7	103.1 ± 1.9	106 ± 10	761 ± 83	2.3 ± 0.5	7.4 ± 0.3	3.2 ± 0.5	7.5 ± 0.3	0.82 ± 0.14	0.02 ± 0.04
Fat fed	103.8 ± 2.6	104.2 ± 2.3	109 ± 8	782 ± 93	0.3 ± 0.1	5.8 ± 0.6	1.8 ± 0.2	6.0 ± 0.7	1.34 ± 0.12	0.15 ± 0.12
P	NS	NS	NS	NS	$P < 0.01$	$P < 0.05$	$P < 0.05$	$P < 0.05$	$P < 0.05$	NS

Data are means ± SE. Two groups of dogs were compared: the control group after 3 weeks on a control diet (control) and the fat-fed group after 12 weeks on a hypercaloric high-fat diet (fat fed). The results of two steady-state clamp periods with different insulin infusion rates are indicated (0.2 and 1.2 $mU \cdot min^{-1} \cdot kg^{-1}$). Glucose infusion rate, uptake, and production determined from [3-^{3}H]glucose tracer analysis.

control high insulin 482 ± 72 pmol/l; fat-fed low insulin 44 ± 5 pmol/l, fat-fed high insulin 400 ± 71 pmol/l) were in a steady state in both groups of animals. Mean arterial pressure remained unchanged with insulin stimulation and was comparable between control and fat-fed animals (data not shown).

DISCUSSION

Insulin exerts vascular and microvascular actions in insulin-sensitive tissues. In a recent study we showed that insulin, at physiological concentrations, stimulates the extravascular distribution volume of inulin, a 5-kDa polysaccharide. Presumably under the control of insulin, macromolecules of sizes similar to inulin (and presumably insulin itself) gain access to insulin-sensitive nutritive tissues (8). Thus, insulin could enhance its own ability to access sensitive tissues. Therefore, supporting previous work by Baron and colleagues (1,2) and Clark et al. (10), hemodynamic effects of insulin could play an important role in insulin action.

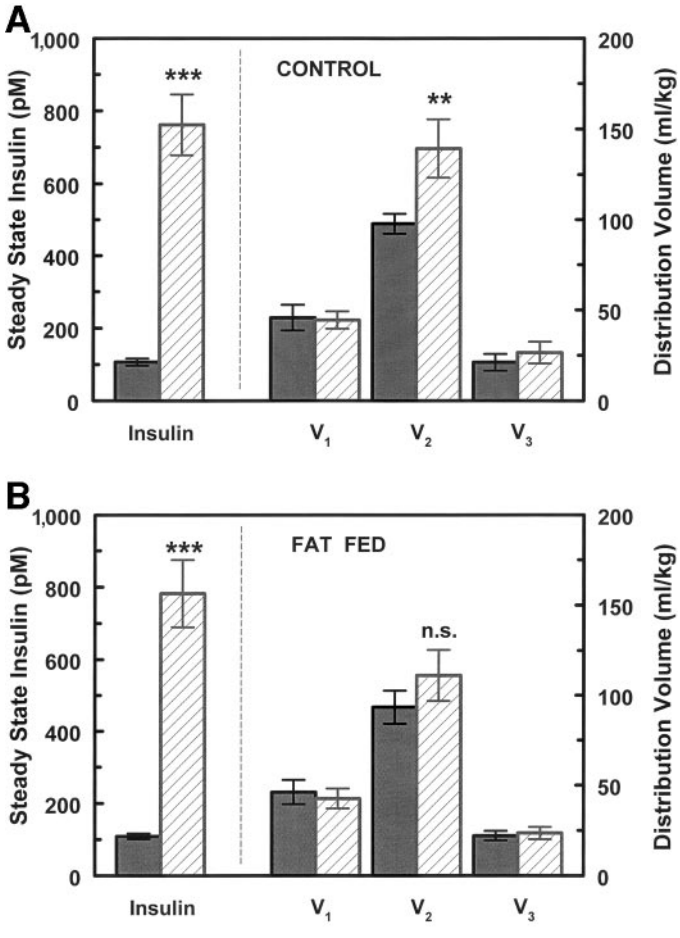

FIG. 2. Results from study 2. Steady-state plasma insulin concentrations and model-predicted distribution volumes during low (■) and physiologically elevated (▨) insulin infusion. *A*: Data from control experiments. *B*: Data from dogs after 12 weeks on a hypercaloric high-fat diet. Data are means ± SE.

The question addressed in the present study was whether a physiologically based insulin resistance (due to fat feeding) would alter this hemodynamic effect of insulin. Our results from two independently performed protocols demonstrate a sizeable reduction of the peripheral macromolecular distribution volume after diet-induced insulin resistance. There was no substantial effect of the high-fat diet on vascular distribution volume or fractional clearance from the plasma compartment. The present results show that the delivery of macromolecules to peripheral tissues is diminished during diet-induced insulin resistance. Considering that these peripheral tissues are likely insulin sensitive, the delivery of insulin itself could be defective with obesity, and this defect will contribute quantitatively to the development of peripheral insulin resistance. This defect would presumably synergize with insulin downregulation at the cellular level (i.e., on insulin signaling at skeletal muscle) to exacerbate overall whole-body insulin resistance.

In previous studies (11,19) we used an isocaloric elevated-fat diet to investigate metabolic changes longitudinally over a period of 12 weeks. With this previous moderate-fat diet, animals demonstrated hepatic, but not peripheral, insulin resistance. However, the diet for the present study was hypercaloric and enriched with triple the amount of added cooked bacon grease (6 g/kg per day). This enrichment was well tolerated and, by observation, enjoyed by the animals on a voluntary basis. As a result, dogs easily gained significant weight, total trunk fat almost doubled, and we observed substantial peripheral as well as hepatic resistance to insulin. Despite overall insulin resistance, and similar to previous studies using an isocaloric fat diet, dogs on the present hypercaloric diet did not develop fasting hyperglycemia, but they did demonstrate substantial fasting hyperinsulinemia to compensate for insulin resistance. The signal(s) responsible for hyperinsulinemia in the face of increased fat storage and insulin resistance remains to be delineated.

It is well known that cellular defects of insulin at the postreceptor level have a substantial impact on the development of insulin resistance. But, the overall development of diet-induced insulin resistance has not been associated with a single biochemical defect (20). To the plethora of

TABLE 5
Model parameters for study 2: results of hyperinsulinemic-euglycemic clamp experiments in anesthetized dogs

	V_1 (ml/kg)	V_2 (ml/kg)	V_3 (ml/kg)	CL_{01} (ml/min)	CL_2 (ml/min)	CL_3 (ml/min)
Low insulin	**46 ± 7** (46 ± 7)	**93 ± 9** (98 ± 6)	**22 ± 3** (21 ± 5)	**95 ± 7** (91 ± 9)	**84 ± 13** (78 ± 8)	**200 ± 39** (211 ± 66)
High insulin	**43 ± 6** (44 ± 5)	**111 ± 14** (139 ± 16)	**24 ± 3** (27 ± 6)	**87 ± 7** (87 ± 10)	**75 ± 11** (80 ± 10)	**207 ± 26** (219 ± 61)
Δ (%)	**−7** (−1)	**18** (32)	**6** (18)	**−8** (−1)	**−11** (13)	**11** (19)
P	**NS** (NS)	**NS** ($P < 0.01$)	**NS** (NS)	**NS** (NS)	**NS** (NS)	**NS** (NS)

Data are means ± SE. Compartment model analysis for two different insulin clamp levels are indicated (low insulin 0.2 mU · min^{-1} · kg^{-1} and high insulin 1.2 mU · min^{-1} · kg^{-1}). Results from dogs after 12 weeks on a high-fat diet are indicated in bold; results after 3 weeks on a control diet are in parentheses. CL_{01}, CL_2, and CL_3 indicate clearance and tissue-specific transport.

possible intracellular defects that have been suggested as playing a role in insulin resistance (21), we can add that the delivery of insulin itself to insulin-sensitive tissues may well be an additional mechanism of insulin resistance. Baron et al. (22) championed the concept that insulin stimulated blood flow to sensitive tissues (23), but the validity of this mechanism has been questioned (24). As an alternative, Clark and Barrett and colleagues (6,9,25) have obtained compelling evidence to suggest that insulin acts by altering the distribution of blood flow from so-called nonnutritive (e.g., tendons and skin) to nutritive (e.g., muscle) tissues. The present results indicate an effect of fat feeding on insulin's ability to alter macromolecular distribution of diffusionary markers to insulin-sensitive tissues. The present results are consistent with the model of Clark and colleagues; that is, insulin alters distribution of capillary access from insulin-independent tissues supplying a limited interstitial space to insulin-dependent tissues such as muscle with a substantial interstitial distribution space associated with the slow distribution volume of macromolecules including insulin. Of course, it is of interest to ask whether the slow compartment is related to insulin-sensitive tissues. Skeletal muscle accounts for most of the insulin-sensitive tissue in the lean individual. In addition, while fenestrations exist for liver tissue, allowing rapid equilibration of large molecules including insulin to the liver, muscle capillaries have limited permeability for large molecules. It is therefore reasonable to conclude that the slowly equilibrating compartment of the present distribution model equates, at least in part, with skeletal muscle tissue. Therefore, reducing movement into this compartment of larger peptides including insulin will invariably lead to whole-body insulin resistance, as insulin will be less able to access those tissues where it is active. Of course, as the present studies only examined the distribution of inulin, which is an imperfect (i.e., uncharged, not folded) analog for insulin, it remains to be proven that insulin itself is less able to access skeletal muscle tissue. However, as transendothelial transport of insulin is a passive process (26), it is unlikely that insulin would be able to access tissues that inulin cannot.

In a recent study by Kim et al. (27), a possible link between obesity and insulin resistance with vascular dysfunction and inflammation was proposed and evidenced. Kim et al. reported that elevated free fatty acid levels activate inhibitor of κβ kinase in endothelial cells, inhibiting nitric oxide (NO) production, and thus might stimulate additional pathways responsible for the development of endothelial dysfunction. In another study, it has been shown that insulin stimulates capillary recruitment by stimulating flow to the microvasculature in skeletal muscle via a NO-dependent pathway. In their study, Vincent et al. (28) have also indicated that inhibition of this pathway is able to blunt glucose uptake in skeletal muscle in response to insulin. Whether this described defect as shown in a rat hindlimb preparation is a possible mechanism for the effect as seen in the present investigations remains speculative. Furthermore, more mechanistic studies will be required to address this hypothesis.

An important question is the relative contribution of changes in access to insulin-sensitive tissues versus mobilization of GLUT4 to the action of insulin. In lean animals, insulin increased volume of the slowly equilibrating compartment by 40%. This effect was substantially reduced with fat feeding. Clearly, if the only effect of insulin on glucose utilization were stimulation of GLUT4 mobilization by insulin, we might assume that the increase in glucose uptake in animals on a normal diet was due to the insulin-signaling effect on skeletal muscle. With basal glucose uptake of ~3 mg · min^{-1} · kg^{-1}, the increase in glucose uptake in animals on normal diet is ~9 mg · min^{-1} · kg^{-1} compared with those on a high-fat diet, which is ~5 mg · min^{-1} · kg^{-1}. However, because the distribution volume increased by 40%, some proportion of the stimulation of uptake is due to an increase in access of insulin-sensitive tissues. Thus, we can assume that the effect of insulin to stimulate uptake may be approximated by the following relationship:

Insulin-stimulated glucose uptake (*ISGU*) = distribution space of insulin-sensitive tissues × increase in uptake per cell (ΔU), or

$$ISGU = V_2 \cdot \Delta U \quad (4)$$

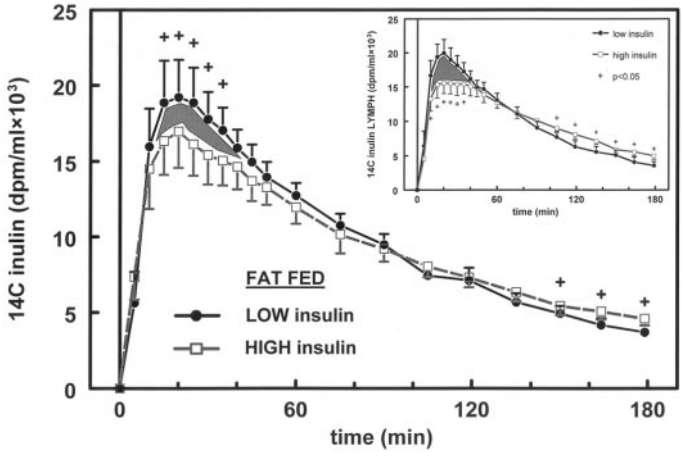

FIG. 3. Results from study 2. Response of the interstitial fluid compartment of skeletal muscle as represented by the hindlimb lymph compartment for low (●) and physiologically elevated (□) insulin concentrations. Major graph indicates insulin response after 12 weeks on a hypercaloric high-fat diet (fat fed), small graph indicates insulin responses in dogs on a control diet (control). Hatched areas indicate smaller difference between interstitial fluid responses for fat-fed (major graph) versus control (small graph) animals. All data are presented as means ± SE.

In the fat-fed situation

$$ISGU_f = V_{2f} \cdot \Delta U_f \quad (5)$$

where the subscript *f* refers to the fat-fed condition. The relative increase in glucose uptake per cell due only to the insulin-signaling effects on insulin-sensitive tissues can be approximated by

$$\frac{\Delta U}{\Delta U_f} = \frac{ISGU}{ISGU_f \cdot (V_2/V_{2f})}$$

$$\frac{\Delta U}{\Delta U_f} = \frac{9\ \text{mg} \cdot \text{min}^{-1} \cdot \text{kg}^{-1}}{5\ \text{mg} \cdot \text{min}^{-1} \cdot \text{kg}^{-1} \times 1.4} \quad (6)$$

Thus, we can estimate that stimulation of glucose transport at the cellular level increased glucose uptake 1.3-fold in healthy animals and that increased distribution into insulin-sensitive tissues increased the uptake from 1.3- to 1.8-fold. Thus, of the reduction of insulin stimulation of glucose uptake from 9 to 5 mg $\cdot$ min^{-1} $\cdot$ kg^{-1}, this is composed of decreasing the effects of insulin on the sensitive tissues (i.e., skeletal muscle) by ~23%, and the additional reduction of another 22% is due to the reduction in distribution volume. Therefore, we speculate that the observed defect of insulin on the distribution volume may have an equivalent contribution to the development of peripheral insulin resistance as the intracellular effects on insulin-sensitive tissues such as skeletal muscle.

From two separately performed studies, the present results support a novel and indeed quantitatively important mechanism that will contribute to the development of obesity-related insulin resistance. While the role of the observed defect on metabolic actions of insulin is likely to be important in the pathogenesis of insulin resistance, the metabolic syndrome, and diabetes, the exact mechanism remains unknown and remains to be investigated.

ACKNOWLEDGMENTS

This work was supported by grants from Novo Nordisk and the National Institutes of Health (DK 27619 and DK 29867). S.P.K. was supported by a predoctoral training grant from the National Institute of Aging (T32-AG-00093).

The authors thank Elza Demirchyan for technical assistance.

REFERENCES

1. Baron AD: Hemodynamic actions of insulin. *Am J Physiol* 267:E187–E202, 1994
2. Steinberg HO, Baron AD: Vascular function, insulin resistance and fatty acids. *Diabetologia* 45:623–634, 2002
3. Liang C, Doherty JU, Faillace R, Maekawa K, Arnold S, Gavras H, Hood WB Jr: Insulin infusion in conscious dogs: effects on systemic and coronary hemodynamics, regional blood flows, and plasma catecholamines. *J Clin Invest* 69:1321–1336, 1982
4. James DE, Burleigh KM, Storlien LH, Bennett SP, Kraegen EW: Heterogeneity of insulin action in muscle: influence of blood flow. *Am J Physiol* 251:E422–E430, 1986
5. Anderson EA, Hoffman RP, Balon TW, Sinkey CA, Mark AL: Hyperinsulinemia produces both sympathetic neural activation and vasodilation in normal humans. *J Clin Invest* 87:2246–2252, 1991
6. Clark MG, Wallis MG, Barrett EJ, Vincent MA, Richards SM, Clerk LH, Rattigan S: Blood flow and muscle metabolism: a focus on insulin action. *Am J Physiol Endocrinol Metab* 284:E241–E258, 2003
7. Bonadonna RC, Saccomani MP, Del Prato S, Bonora E, DeFronzo RA, Cobelli C: Role of tissue-specific blood flow and tissue recruitment in insulin-mediated glucose uptake of human skeletal muscle. *Circulation* 98:234–241, 1998
8. Ellmerer M, Kim SP, Hamilton-Wessler M, Hucking K, Kirkman E, Bergman RN: Physiological hyperinsulinemia in dogs augments access of macromolecules to insulin-sensitive tissues. *Diabetes* 53:2741–2747, 2004
9. Rattigan S, Clark MG, Barrett EJ: Hemodynamic actions of insulin in rat skeletal muscle: evidence for capillary recruitment. *Diabetes* 46:1381–1388, 1997
10. Clark MG, Colquhoun EQ, Rattigan S, Dora KA, Eldershaw TP, Hall JL, Ye J: Vascular and endocrine control of muscle metabolism. *Am J Physiol* 268:E797–E812, 1995
11. Kim SP, Ellmerer M, Van Citters GW, Bergman RN: Primacy of hepatic insulin resistance in the development of the metabolic syndrome induced by an isocaloric moderate-fat diet in the dog. *Diabetes* 52:2453–2460, 2003
12. Finegood DT, Bergman RN, Vranic M: Estimation of endogenous glucose production during hyperinsulinemic-euglycemic glucose clamps: comparison of unlabeled and labeled exogenous glucose infusates. *Diabetes* 36:914–924, 1987
13. Poulin RA, Steil GM, Moore DM, Ader M, Bergman RN: Dynamics of glucose production and uptake are more closely related to insulin in hindlimb lymph than in thoracic duct lymph. *Diabetes* 43:180–190, 1994
14. Yang YJ, Hope ID, Ader M, Bergman RN: Insulin transport across capillaries is rate limiting for insulin action in dogs. *J Clin Invest* 84:1620–1628, 1989
15. Krebs M, Stingl H, Nowotny P, Weghuber D, Bischof M, Waldhausl W, Roden M: Prevention of in vitro lipolysis by tetrahydrolipstatin. *Clin Chem* 46:950–954, 2000
16. Henthorn TK, Avram MJ, Frederiksen MC, Atkinson AJ Jr: Heterogeneity of interstitial fluid space demonstrated by simultaneous kinetic analysis of the distribution and elimination of inulin and gallamine. *J Pharmacol Exp Ther* 222:389–394, 1982
17. Steil GM, Meador MA, Bergman RN: Thoracic duct lymph: relative contribution from splanchnic and muscle tissue. *Diabetes* 42:720–731, 1993
18. Sedek GS, Ruo TI, Frederiksen MC, Frederiksen JW, Shih SR, Atkinson AJ Jr: Splanchnic tissues are a major part of the rapid distribution spaces of inulin, urea and theophylline. *J Pharmacol Exp Ther* 251:1026–1031, 1989
19. Mittelman SD, Van Citters GW, Kim SP, Davis DA, Dea MK, Hamilton-Wessler M, Bergman RN: Longitudinal compensation for fat-induced insulin resistance includes reduced insulin clearance and enhanced beta-cell response. *Diabetes* 49:2116–2125, 2000
20. Saltiel AR, Kahn CR: Insulin signalling and the regulation of glucose and lipid metabolism. *Nature* 414:799–806, 2001
21. Elmquist JK, Marcus JN: Rethinking the central causes of diabetes. *Nat Med* 9:645–647, 2003
22. Baron AD, Tarshoby M, Hook G, Lazaridis EN, Cronin J, Johnson A, Steinberg HO: Interaction between insulin sensitivity and muscle perfusion on glucose uptake in human skeletal muscle: evidence for capillary recruitment. *Diabetes* 49:768–774, 2000
23. Laakso M, Edelman SV, Brechtel G, Baron AD: Decreased effect of insulin to stimulate skeletal muscle blood flow in obese man: a novel mechanism for insulin resistance. *J Clin Invest* 85:1844–1852, 1990
24. Yki-Jarvinen H, Utriainen T: Insulin-induced vasodilatation: physiology or pharmacology? *Diabetologia* 41:369–379, 1998
25. Vincent MA, Dawson D, Clark AD, Lindner JR, Rattigan S, Clark MG, Barrett EJ: Skeletal muscle microvascular recruitment by physiological hyperinsulinemia precedes increases in total blood flow. *Diabetes* 51:42–48, 2002
26. Hamilton-Wessler M, Ader M, Dea MK, Moore D, Loftager M, Markussen J, Bergman RN: Mode of transcapillary transport of insulin and insulin analog NN304 in dog hindlimb: evidence for passive diffusion. *Diabetes* 51:574–582, 2002
27. Kim F, Tysseling KA, Rice J, Pham M, Haji L, Gallis BM, Baas AS, Paramsothy P, Giachelli CM, Corson MA, Raines EW: Free fatty acid impairment of nitric oxide production in endothelial cells is mediated by IKKbeta. *Arterioscler Thromb Vasc Biol* 25:989–994, 2005
28. Vincent MA, Barrett EJ, Lindner JR, Clark MG, Rattigan S: Inhibiting NOS blocks microvascular recruitment and blunts muscle glucose uptake in response to insulin. *Am J Physiol Endocrinol Metab* 285:E123–E129, 2003